The British Journal of Radiology, 85 (2012), 729–735

Serial evaluation of high-resolution CT findings in patients with pneumonia in novel swine-origin influenza A (H1N1) virus infection

[1]P LI, PhD, [1]J-F ZHANG, BSc, [1]X-D XIA, MSc, [2]D-J SU, PhD, [1]B-L LIU, [1]D-L ZHAO, [3]Y LIU, PhD and [4]D-H ZHAO

[1]*Department of Radiology, the Second Affiliated Hospital of Harbin Medical University, Harbin, China,* [2]*Department of Respiratory Medicine, the Second Affiliated Hospital of Harbin Medical University, Harbin, China,* [3]*The Department of Statistics, Harbin Medical University, Harbin, China, and* [4]*Centers for Disease Control and Prevention of Heilongjiang, Harbin, China*

Objectives: The purpose of our study was to review the changes in the serial high-resolution CT (HRCT) findings from patients with novel swine-origin influenza A (H1N1) virus (S-OIV) infection.
Methods: HRCT findings of 70 patients with presumed or laboratory-confirmed novel S-OIV infection were reviewed. The pattern (consolidation, ground glass, fibrosis and air trapping), distribution and extent of abnormality of the lesions on the HRCT were evaluated at different time points. To assess changes that occurred over time, the CT scans in 56 patients were examined in sequence.
Results: The most common CT findings in patients with S-OIV infection are ground-glass opacities with or without consolidation at the first week. The abnormalities peaked at the second week and resolved after that time, which resulted in substantial reduced residual disease at 4 weeks or later. The development of fibrosis was noted in the first week and peaked at the third week of illness (34.7%), then decreased slowly after that time. The mean time of air trapping being noted after the onset of symptoms was 55.5 ± 20.6 days. Comparing the findings of initial CT, most results (96.4%) of follow-up chest CT findings showed improvement ($p < 0.01$).
Conclusion: The abnormalities of ground-glass opacities and/or consolidation on initial CT scans tended to resolve to fibrosis, which then resolved completely or displayed substantially reduced residual disease. HRCT may show more changes in disease progression and play an important role in the evaluation of severe S-OIV.

Received 29 June 2010
Revised 17 January 2011
Accepted 31 January 2011

DOI: 10.1259/bjr/85580974

A novel swine-origin influenza A (H1N1) virus (S-OIV) was first reported in Mexico and became rampant globally later on in spring 2009 [1]. The World Health Organization declared the first Phase 6 global influenza pandemic of the century on 11 June 2009 [2]. During peak periods of influenza in autumn to winter of that year, a proportion of patients developed severe acute respiratory distress syndrome (ARDS), and some died of the disease. Serial chest radiography has been the main technique in the initial investigation of patients with suspected H1N1. However, multislice CT (MSCT) scanning is more sensitive than chest radiography, providing more detailed radiological features. Previous studies have reported that the predominant CT findings of disease were unilateral or bilateral multifocal peribronchovascular and/or subpleural ground-glass opacities (GGOs) with or without consolidation [1, 3]. Little is known, however, about sequential MSCT findings during the subsequent course of pneumonia with H1N1. The purpose of this study was to evaluate the radiological changes on serial thin-section chest CT scans in patients with H1N1 during the acute and convalescent periods of the illness.

Address correspondence to: Dr Ping Li, Department of Radiology, the Second Affiliated Hospital of Harbin Medical University, 246 Xue Fu Road, Harbin 150086, China. E-mail: pinglee_2000@yahoo.com

Methods and materials

Subjects

We retrospectively reviewed 70 patients hospitalised with presumed or laboratory-confirmed novel S-OIV (H1N1) infection who underwent initial thin-section CT scans of the thorax from October 2009 to January 2010 (36 males and 34 females; 3–71 years of age, 33.8 ± 15.1 years on average). 64 of the 70 patients had no significant medical history, including 8 patients who were pregnant. 38 of these patients were confirmed to have S-OIV (H1N1) by testing respiratory specimens with real-time reverse transcription polymerase chain reaction (RT-PCR) at Centers for Disease Control and Prevention (CDC) in China [4]. The 70 patients were divided into two groups. Group 1 consisted of 29 critically ill patients. Critically ill patients were defined as (1) those admitted to an intensive care unit (ICU) or those requiring mechanical ventilation (invasive or non-invasive) and (2) those with a fraction of inspired oxygen (F_IO_2)

concentration greater than or equal to 60%. Group 2 consisted of 41 patients who required brief hospitalisation without advanced mechanical ventilation but were administered drugs.

CT techniques

Thin-section MSCT was performed for all 70 patients on a 10-slice scanner (Sensation 10; Siemens Healthcare, Munich, Germany) or 16-slice multidetector CT (MDCT) scanner (Lightspeed 16; GE Healthcare, Little Chalfont, UK). The protocol used was as follows: end-inspiratory acquisition, 120 kV, 150~200 mAs, and 2 mm reformation. The images were viewed on both lung (window width, 1400 HU; level, –700 HU) and mediastinal (window width, 350 HU; level, 40 HU) settings. The reconstructions were made at 2 mm slice thickness on lung settings. All examinations were performed with the patients in the supine position holding their breath during inspiration without iv contrast administration. All 29 patients in the ICU had serial bedside anteroposterior-projection follow-up radiographs.

Image analysis

Two experienced radiologists with thoracic imaging experience of 12 and 14 years reviewed MDCT scans independently and reached a decision on the final interpretations by consensus. Thin-section CT findings were recorded, including GGO, consolidation, nodular opacities, reticulation, parenchymal bands, air trapping, bronchiectasis, irregular linear opacities and interfaces. The presence of parenchymal bands, irregular linear opacities, interfaces and traction bronchiectasis was considered evidence of probable fibrosis. GGOs were defined as hazy areas of increased opacity or attenuation without concealing the underlying vessels. Consolidation was defined as homogeneous opacification of the parenchyma with obscuration of the underlying vessels. Nodular opacities were defined as focal round opacities. Reticular opacities were defined as linear opacities forming a mesh-like pattern. Parenchymal bands were defined as non-tapering linear opacities a few millimetres thick and several centimetres long. Air trapping was defined as an area of low attenuation in contrast with the background attenuation of lung parenchyma on images obtained during expiration. The presence of mediastinal lymphadenopathy (defined as a lymph node $\geq$1 cm in short-axis diameter), pneumothorax, pneumomediastinum and pleural effusion was also noted.

The date of symptom onset and the date of initial CT scans of all the patients were recorded. After evaluation, all scans were categorised according to the time between these two time points at 1, 2, 3, 4 or longer than 4 weeks after onset of symptoms. To assess changes that occurred over time, the CT scans in some patients were examined in sequence. Patients with initial and follow-up scans were selected for assessment of changes in lung abnormalities. The patterns, extent and distribution of abnormal CT findings were compared with findings in the same region on previous and subsequent CT scans.

The extent of involvement of each abnormality was assessed independently for each of three zones: upper (above the carina), middle (below carina up to the inferior pulmonary vein) and lower (below the inferior pulmonary vein). Each lung zone (total of six lung zones) was assigned a score, modified from the previously described protocol [5] and based on the following: 0 when no involvement, 1 when <25% involvement, 2 when 25–50% involvement; 3 when 50–75% involvement and 4 when >75% involvement. Summation of scores provided overall lung involvement (maximal CT score=24).

Statistical analysis

All data are expressed as mean $\pm$ standard deviation (SD) unless otherwise indicated. For categorical variables, the percentages of patients in each category were calculated. A p-value <0.05 was considered to indicate a statistically significant difference. Differences in the two groups were tested by using χ^2 statistics. Observer variations were evaluated using the kappa coefficient for semi-categorical variables. To compare the difference in time course of CT scores between two groups, profile analysis was used by means of a repeated-measures analysis of variance (ANOVA) model. Changes in score between the first and last thin-section CT examinations were compared by using a Wilcoxon signed-rank test. All of the data were analysed with statistical software (SPSS, version 13.0; SPSS Inc., Chicago, IL).

Results

Serial thin-section CT findings in patients with H1N1

There was no age difference between the two groups defined in the materials and methods ($p>0.05$). The initial thin-section CT examination was performed at 17.2 $\pm$ 19.7 days (mean $\pm$ SD; range 1–32 days) after onset of H1N1 symptoms in the 70 patients.

The predominant radiographic findings in the 70 patients at presentation were unilateral or bilateral multifocal asymmetric GGOs with or without bilateral consolidation (Figure 1), which were similar to those described in other reports [6]. GGOs alone or with superimposed consolidation were predominant in the first week and decreased thereafter (Figure 2; Table 1). At the first week after onset of symptoms, GGOs were noted in 95% (38/40) of patients and consolidation was noted in 57.5% (23/40) of patients. The most common pattern observed in initial CT scans was GGOs alone in Group 2 patients (51.2%; 21/41) and GGOs with superimposed consolidation in Group 1 patients (62.9%; 18/29), but the difference of their patterns was not significant between the groups ($p>0.05$). Smooth intralobular lines, reticular opacities, mild traction bronchiectasis, parenchymal bands, irregular linear opacities and interfaces, which suggested fibrosis, were noted in the first week after onset of symptoms and increased. By the second week, the greatest number of smooth intralobular lines and other superimposed reticular opacities were noted in association with GGOs (Figure 2). Thickening of

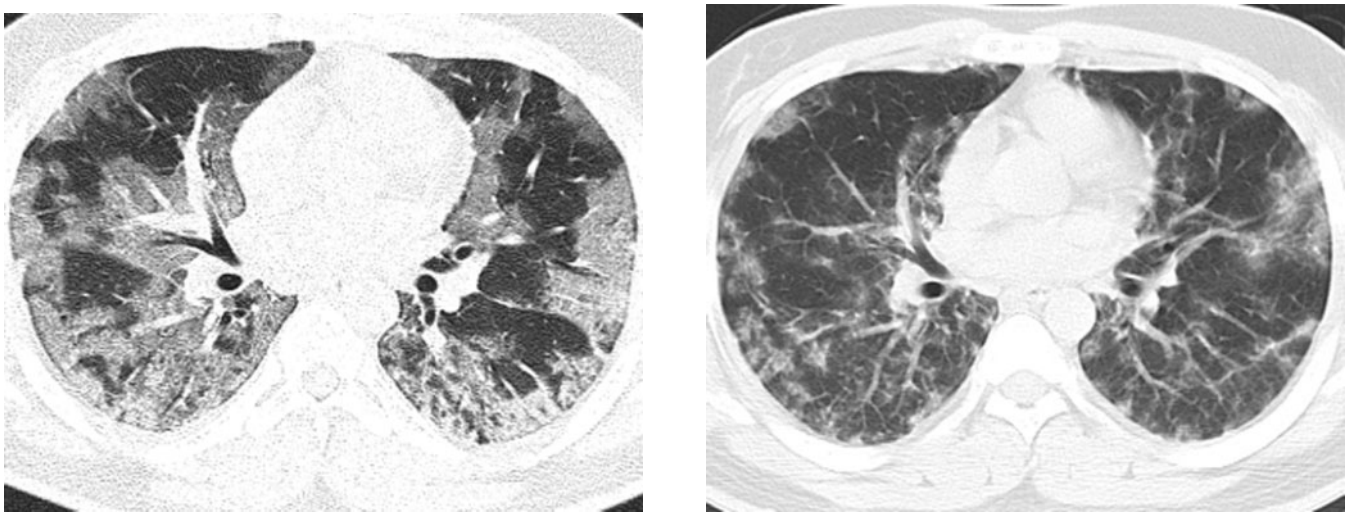

(a) (b)

Figure 1. Transverse thin-section CT scans in 27-year-old male with presumed H1N1. (a) Scan obtained on day 7 of illness shows diffuse peripheral distribution of ground-glass opacities (GGOs). (b) Scan obtained on day 14 of illness shows irregular linear opacities that developed in the areas of GGOs.

interlobular septa and intralobular lines in both sides can also be seen at the second week. The mean time of fibrosis being observed was 22.7 ± 15.8 days after the onset of symptoms. The sign of air trapping was only seen in nine patients who received prolonged ventilation and was not seen in patients who had never received ventilation or who had received ventilation for only a short time. Most of the air trapping was located in the ventral lung, which is normal before mechanical ventilation, and was observed after 4 weeks (Figure 3). The mean time of air trapping noted after the onset of symptoms was 55.5 ± 20.6 days. However, further follow-up in these patients is required to determine whether these changes are reversible.

4 (5.5%) of the 70 patients developed pneumomediastinum that was only evident on high-resolution CT. 15 (21%) of the 70 patients had small bilateral or unilateral pleural effusions. Pleural effusions decreased gradually on follow-up CT. None had evidence of hilar or mediastinal lymph node enlargement on CT performed at admission or later.

Changes of serial thin-section CT features

Serial thin-section CT scans obtained between the time of initial and final scans were obtained in 56 patients. Compared with the initial CT, the final CT findings showed most of these patients (54 of 56 patients, 96.4%) had improved ($p<0.001$; Figure 4). 2 of 56 patients died of ARDS. The disease extent was greater in group 1 patients requiring advanced mechanical ventilation at the time of the initial CT scan, and scores were higher for Group 1 than for Group 2 patients in each week after symptom onset ($p<0.001$ for all; Table 2). Interobserver agreement for scoring CT abnormality for all scans was 0.879. Two-way repeated-measures ANOVA revealed significant between-subject effects for the two groups ($p<0.001$), and for the interaction between scores and groups ($p<0.001$). There was a marked increase in disease extent during the second week of illness and the estimated marginal mean CT score peaked in week 2 of illness in both groups, with a slow decrease thereafter (Figure 5). The curves are approximately parallel for the two groups,

(a) (b) (c)

Figure 2. Transverse thin-section CT scans in 34-year-old pregnant female with laboratory-confirmed swine-origin influenza A (H1N1) virus. (a) Scan obtained on the day of the onset of fever shows ground-glass opacities (GGOs) peribronchovascular and subpleural predominance. (b) Scan obtained on day 5 of illness shows that the opacities became larger and thicker on the same level as (a). (c) Scan obtained on day 9 of illness shows irregular linear opacities that developed in the areas of GGOs and mild traction bronchiectasis (arrow).

Table 1. The patterns of abnormality of the lesions on the high-resolution CT at the different weeks

Week	Ground-glass opacities	Consolidation	Fibrosis	Air trapping
1 (n=40)	38 (95%)	23 (57.5%)	5 (12.5%)	0 (0%)
2 (n=54)	43 (79.6%)	25 (46.3%)	16 (29.6%)	0 (0%)
3 (n=31)	10 (32.3%)	12 (38.7%)	25 (80.6%)	0 (0%)
4 (n=15)	6 (40%)	6 (40%)	12 (80%)	0 (0%)
>4 (n=18)	8 (44.4%)	4 (22.2%)	14 (77%)	9 (50%)

although the scores are higher for Group 1 than for Group 2 in each week ($p<0.001$).

Discussion

Swine influenza is a highly contagious acute respiratory disease of pigs caused by a subtype of influenza A virus. The most common clinical symptoms at presentation are fever, cough, dyspnoea and respiratory distress [7]. Although most cases of H1N1 virus (S-OIV) have been self-limiting, fatal cases raise questions about virulence and radiology's role in detection. Pneumonia is one of the most common complications of H1N1 influenza and results in the majority of fatal outcomes in the world [8, 9].

H1N1 influenza is still a novel disease, with poorly understood pathology and pathogenesis. The histological changes of pneumonia in H1N1 are characteristic of influenza, though not pathognomonic. Autopsies have shown that the main pathological changes associated with S-OIV infection are localised to the lungs [10]. The lungs typically show focal to extensive diffuse alveolar damage (DAD) [11, 12]. In the early exudative inflammatory phase of the disease (<10–12 days), DAD is predominant. The early or exudative stage is characterised by pulmonary oedema with hyaline membranes, alveolar septal oedema, fibrin thrombus in the vascular lumen and acute pulmonary haemorrhage, which contribute to some typical radiological manifestations such as GGOs and consolidations [12]. Initial CT scans in this study showed bilateral multifocal asymmetric GGOs and consolidation distributed predominantly in subpleural and peribronchovascular areas, corroborating previous preliminary reports [13, 14]. Characterisation of GGOs and consolidations are generally pathologically attributable to the partial displacement of air from partial filling of air spaces, thickening of interstitial tissues from fluid or cells, partial alveolar collapse, or increased capillary blood volume [15, 16]. The following additional histopathological features have also been reported: pneumonia foci with intra-alveolar exudates without evidence of bacterial colonies [11]; moderate to marked inflammation of the submucosal glands and ducts with focal epithelial cytonecrosis; tracheitis and bronchitis, focal squamous metaplasia, and submucosal inflammatory infiltrates [12]; pleuritis; interstitial pneumonitis; cytopathic effect in the bronchial and alveolar epithelial cells; and epithelial hyperplasia and squamous metaplasia of the large airways [12].

The intermediate stage begins in the second week and is a transitional period during which oedematous fluid is reabsorbed and proliferative processes begin. In cases with longer disease duration, changes consistent with the fibrous proliferative phase (organising diffuse alveolar damage) and the final fibrotic stage (interstitial fibrosis) have been observed. Fibrous processes begin to appear from the second week and are visible by CT at this stage of ARDS [17]. These processes are manifested radiologically by the appearance of architectural distortions (*i.e.* irregular interfaces and traction bronchiectasis), a reticular pattern (with septal thickening and parenchymal bands) and subpleural cysts [18]. In the present study, the mean time of fibrosis observed was 22.7 ± 15.8 days after the onset of symptoms. More signs of probable fibrosis may become apparent at CT in this study as the consolidation resolves with time. Fibrosis may appear earlier with a prompt treatment after onset of symptoms. It

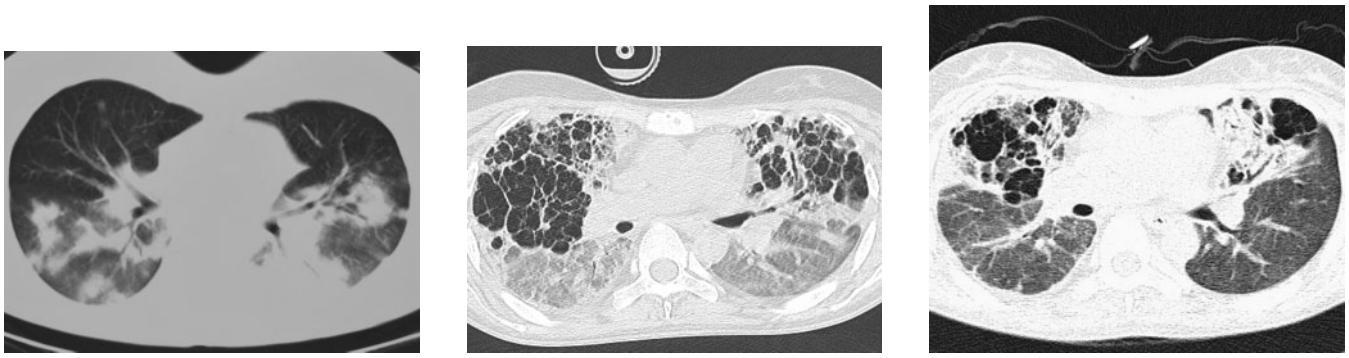

(a) (b) (c)

Figure 3. Transverse scans in 28-year-old pregnant female with laboratory-confirmed swine-origin influenza A (H1N1). (a) Transverse CT scan obtained on day 4 of illness shows ground-glass opacities (GGOs) with bilateral areas of consolidation in mid and lower lung zones. (b) Scan obtained on day 40 of illness shows air trapping developed in the previously normally aerated regions. (c) Scan obtained on day 58 of illness shows that GGOs were resolved, but air trapping persisted.

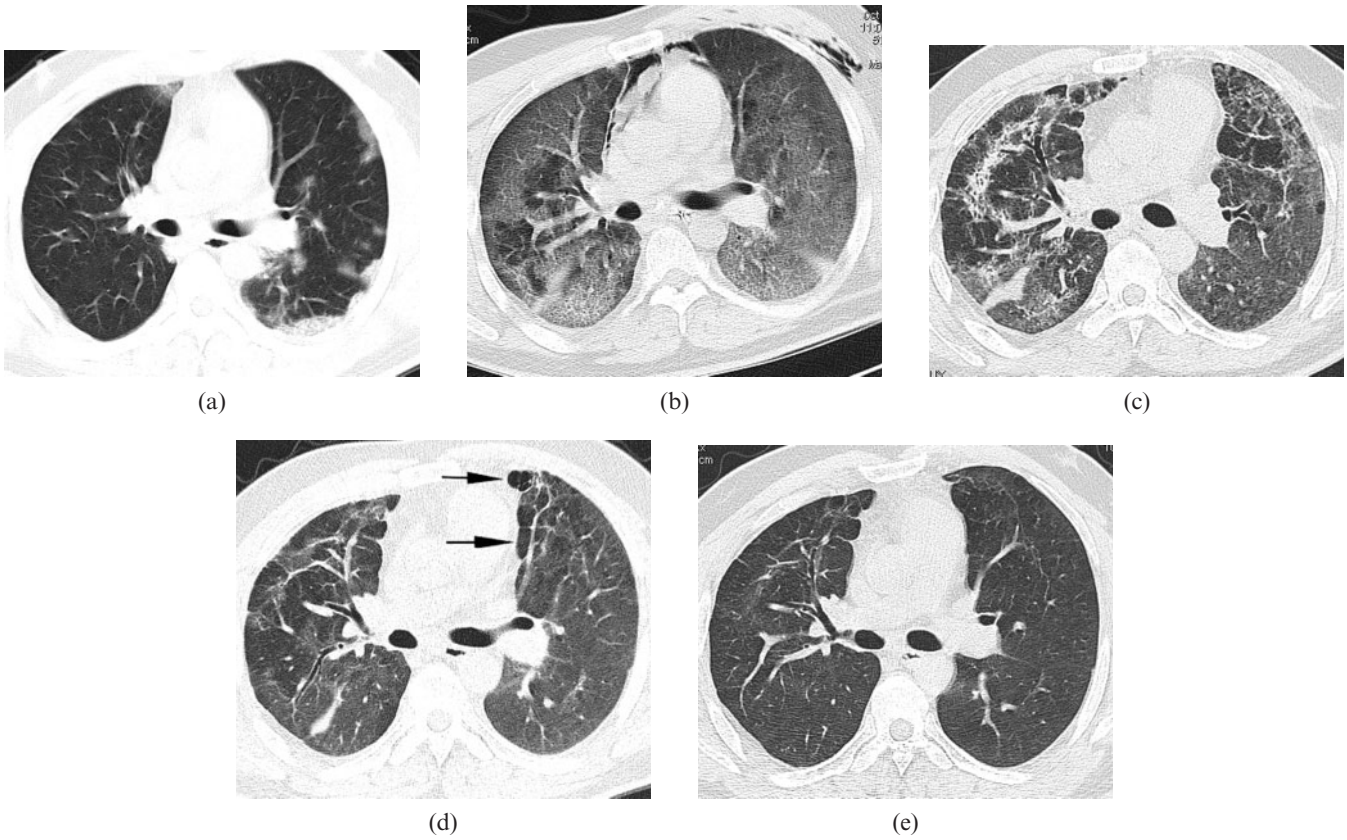

Figure 4. Transverse thin-section CT scans in 34-year-old male with laboratory-confirmed swine-origin influenza A (H1N1). (a) Scan obtained on day 4 of illness shows a peripheral distribution of patchy ground-glass opacities (GGOs). With progression of symptoms, he was admitted to the intensive care unit on the sixth day of illness for mechanical ventilation. (b) Scan obtained on day 10 of illness shows diffuse bilateral GGOs; areas of consolidation predominately in subpleural and dependent lung regions. (c) Scan obtained on day 31 of illness shows irregular linear opacities that developed in the areas of GGOs. (d) Scan obtained on day 64 of illness shows that reticulation superimposed on GGOs persisted, although reduced in extent. Mosaic hypoattenuation (arrows) suggestive of air trapping in the ventral and subpleural lung regions can be seen. (e) Scan obtained on day 195 of illness shows resolution of fibrosis and air trapping.

is difficult to know how many of these structural changes will resolve over time. Further follow-up of these patients would be helpful to understand the evolving process. It is believed that pulmonary fibrosis observed at the recovery phase would, at least in part, account for the respiratory symptoms [19].

As the underlying histopathological features of H1N1 influenza are not unique, it may be difficult to distinguish diffuse alveolar damage caused by H1N1 infections from that caused by other micro-organisms, such as severe acute respiratory syndrome (SARS), coronavirus (SARS-CoV) or avian influenza A (H5N1) [10]. Common features of thin-section CT scan could be found in patients with H1N1, SARS or organising pneumonia [20, 21], particularly during the initial phase of the illness when the GGOs and consolidation are primarily subpleural. Similarly, the presence of smooth interlobular septal thickening superimposed on extensive GGOs can be seen in conditions such as pulmonary alveolar proteinosis, pulmonary oedema and with other types of bacterial or viral pneumonia, such as SARS [22, 23].

The CT findings in cases of S-OIV in this study were found to be similar to those with SARS, as previously reported [24, 25]. In concurrence, we also observed similarity in our group of patients. During the initial phases of both diseases, the viruses cause inflammatory alveolar and interstitial oedema that result in MDCT findings dominated by GGOs [25]. Severe cases can rapidly exhibit radiological and pathological development of diffuse alveolar damage and present with haemoptysis or even ARDS [26]. In addition, both diseases showed no centrilobular nodules, tree-in-bud pattern,

Table 2. The difference of scores between the two groups at the different weeks

Group	Week 1	Week 2	Week 3	Week 4	Week 5
1 (n=25)	14.16±4.77	17.28±5.73	13.08±5.96	10.16±5.91	6.20±4.74
2 (n=31)	8.77±4.50	9.97±5.85	6.45±4.89	3.90±4.18	1.19±1.82
F	18.805	22.028	20.920	21.447	29.321
p-value	<0.001	<0.001	<0.001	<0.001	<0.001

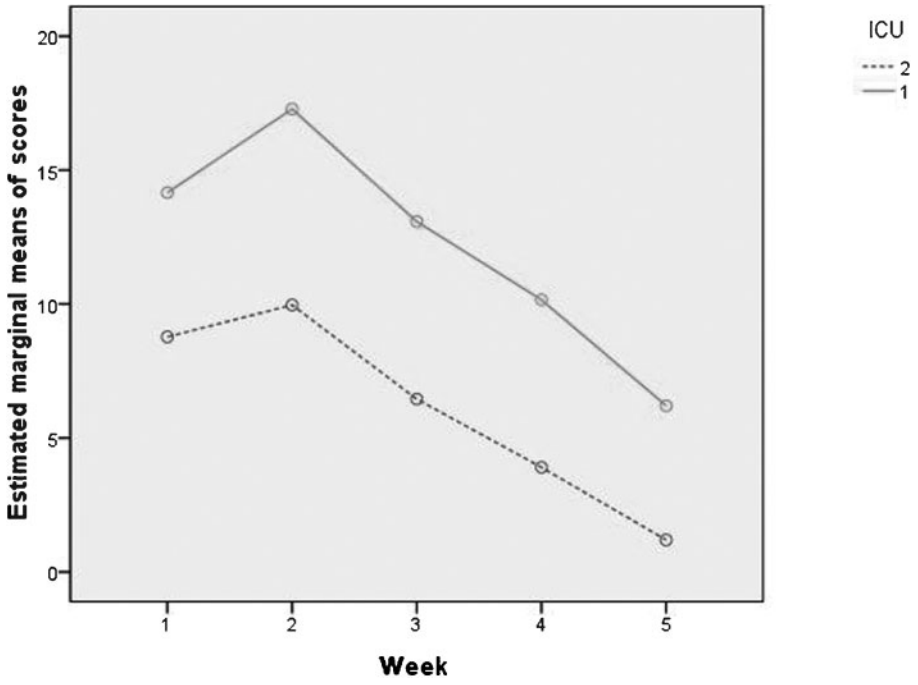

Figure 5. Line graph shows median thin-section CT scores at various time points in weeks after onset of symptoms. Graph shows median thin-section CT scores plotted against mean time for each week for patients admitted to the intensive care unit and those who required brief hospitalisation without advanced mechanical ventilation. The rate of radiographic progression (slope of each curve) for the two groups is roughly parallel over the weeks. There was a marked increase in extent of disease during the second week of illness, and the estimate marginal means of CT score peaked at week 2 of illness in both groups, with a slow decline thereafter.

cavity, or mediastinal or hilar lymphadenopathy [27]. However, 18% of the patients showed pleural effusion, which is different from SARS.

Radiological recovery from H1N1 can be complete, but CT images often show persistent GGO and reticular opacities, some of which reflect pathological findings of fibrosis. Long-term follow-up imaging of survivors shows gradual decrease of GGO and reticulation, with persistent air trapping in some patients. The latter is evidence of small airway disease that cannot be detected on CT scans at the onset of the disease [26]. CT findings manifest as extensive bilateral airspace disease in patients requiring long-term pressure-control mechanical ventilation [28]. Air trapping observed at thin-section CT in our patients was similar to those observed in the late stage of ARDS [29]. Air trapping seen in the present study was not seen in the early stage of the disease or in the patients who did not receive mechanical ventilation, but only in ICU patients with long-term mechanical ventilation, and most of them were seen in the ventral lung [30, 31]. When patients with ARDS receive mechanical ventilation with positive pressure, poorly aerated lobules may be recruited and previously normal aerated regions may become overinflated [18]. It has always been assumed that the changes seen in patients receiving positive pressure ventilation represent a combination of the effects of the primary disease that causes inflammatory changes in the lung parenchyma in addition to the damage caused by prolonged positive-pressure ventilation itself [32]. This suggests that air trapping may be a result of ARDS or a consequence of patients who received long-term mechanical ventilation rather than the inflammatory process. 54 of 56 patients (96.4%) showed improvement in lung fibrotic changes 1 month later. This suggests that the mechanism of lung injury and lung fibrotic changes caused by H1N1 might have a different pathophysiological process compared with other diseases of the lung. H1N1 patients with lung fibrotic changes seem to have the ability for self-rehabilitation, which is similar to SARS cases [33].

This study has several limitations. We evaluated pneumonia patients with presumed/confirmed S-OIV who had serial CT scans upon the initial visit to the hospital as well as after discharge. This group may not be representative of hospitalised patients who were not tested. Despite the use of a standardised data-collection form, not all information was collected for all patients. Another limitation is the different scanning intervals for patients owing to the retrospective nature of the study. In addition, we have no knowledge of the clinical features that prompted outpatient chest radiographic imaging or how these patients differed from patients who did not undergo CT. Future work on correlation between the findings of HRCT with symptoms and pulmonary function and on the effect of drug treatment would provide useful information for a better understanding of the disease and improvements in patient care.

In conclusion, the most common MDCT findings in patients with S-OIV infection are unilateral or bilateral GGOs with or without associated focal or multifocal areas of consolidation at the first week after the onset of symptoms. The abnormalities tended to progress to more extensive GGOs with/without bilateral consolidation, which increased considerably by the second week and resulted in substantially reduced residual disease at 4 weeks or longer after disease onset. Air trapping was only observed in ICU patients who received long-term mechanical ventilation. A small percentage of patients may develop superimposed complications such as pneumothorax and pneumomediastinum, or show reticulation and traction bronchiectasis consistent with fibrosis. Although GGO and interstitial opacity resolve over time, air trapping persists. HRCT may show more changes of parenchymal disease compared with radiographs. Long-term follow-up with thin-section CT and concomitant functional studies are required to determine the long-term pulmonary sequelae of S-OIV.

Acknowledgments

Supported by grants from the National Science and Technology Projects of China (2007C30700189).

We thank Dr Yong Wan, Dr Dan Wang, Dr Hongliang Wang and Dr Yanying Li for their help with the collection of clinical data, Dr Lijuan Zhang, for her careful editing of an earlier version of this article and Dr Yanming Zhao for technical support.

References

1. Perez-Padilla R, de la Rosa-Zamboni D, Ponce de Leon S, Hernandez M, Quiñones-Falconi F, Bautista E, et al. Pneumonia and respiratory failure from swine origin influenza A (H1N1) in Mexico. N Engl J Med 2009;361:680–9.
2. Chan M. World now at the start of 2009 influenza pandemic. Available from: http://www.who.int/mediacentre/news/statements/2009/h1n1_pandemic_phase6_20090611/en/index.html [accessed 20 July 2009].
3. Jain S, Kamimoto L, Bramley AM, Schmitz AM, Benoit SR, Louie J, et al. Hospitalized patients with 2009 H1N1 influenza in the United States, April–June 2009. N Engl J Med 2009;361:1935–44.
4. Cao B, Li XW, Mao Y, Wang J, Lu HZ, Chen YS, et al. Clinical features of the initial cases of 2009 pandemic influenza A (H1N1) virus infection in China. N Engl J Med 2009;361:2507–17.
5. Ooi GC, Khong PL, Müller NL, Yiu WC, Zhou LJ, Ho JC, et al. Severe acute respiratory syndrome: temporal lung changes at thin-section CT in 30 patients. Radiology 2004;230:839–44.
6. Agarwal PP, Cinti S, Kazerooni EA. Chest radiographic and CT findings in novel swine-origin influenza A (H1N1) virus (S-OIV) infection. AJR Am J Roentgenol 2009;193:1488–93.
7. Dawood FS, Jain S, Finelli L, Shaw MW, Lindstrom S, Garten RJ, et al. Emergence of a novel swine-origin influenza a (H1N1) virus in humans. N Engl J Med 2009;360:2605–15.
8. Thompson WW, Shay DK, Weintraub E, Brammer L, Bridges CB, Cox NJ, et al. Influenza-associated hospitalizations in the United States. JAMA 2004;292:1333–40.
9. Harper SA, Bradley JS, Englund JA, File TM, Gravenstein S, Hayden FG, et al. Seasonal influenza in adults and children—diagnosis, treatment, chemoprophylaxis, and institutional outbreak management: clinical practice guidelines of the Infectious Diseases Society of America. Clin Infect Dis 2009;48:1003–32.
10. Mauad T, Hajjar LA, Callegari GD, da Silva LF, Schout D, Galas FR, et al. Lung pathology in fatal novel human influenza A (H1N1) infection. Am J Respir Crit Care Med 2010;181:72–9.
11. Soto-Abraham MV, Soriano-Rosas J, Díaz-Quiñónez A, Silva-Pereyra J, Vazquez-Hernandez P, Torres-López O, et al. Pathological changes associated with the 2009 H1N1 virus. N Engl J Med 2009;361:2001–3.
12. Gill JR, Sheng ZM, Ely SF, Guinee DG, Beasley MB, Suh J, et al. Pulmonary pathologic findings of fatal 2009 pandemic influenza A/H1N1 viral infections. Arch Pathol Lab Med 2010;134:235–43.
13. Li P, Su DJ, Zhang JF, Xia XD, Sui H, Zhao DH. Pneumonia in novel swine-origin influenza A (H1N1) virus infection: high-resolution CT findings. Eur J Radiol 2010;80:e146–52.
14. Ajlan AM, Quiney B, Nicolaou S, Müller NL. Swine-origin influenza A (H1N1) viral infection radiographic and CT findings. AJR Am J Roentgenol 2009;193:1494–9.
15. Remy-Jardin M, Giraud F, Remy J, Copin MC, Gosselin B, Duhamel A. Importance of ground-glass attenuation in chronic diffuse infiltrative lung disease: pathologic-CT correlation. Radiology 1993;189:693–8.
16. Mollura DJ, Asnis DS, Crupi RS, Conetta R, Feigin DS, Bray M, et al. Imaging findings in a fatal case of pandemic swine-Origin influenza A (H1N1). AJR Am J Roentgenol 2009;193:1500–3.
17. Gattinoni L, Bombino M, Pelosi P, Lissoni A, Pesenti A, Fumagalli R, et al. Lung structure and function in different stages of severe adult respiratory distress syndrome. JAMA 1994;271:1772–9.
18. Joynt GM, Antonio GE, Lam P, Wong KT, Li T, Gomersall CD, et al. Late-stage adult respiratory distress syndrome caused by severe acute respiratory syndrome: abnormal findings at thin-section CT. Radiology 2004;230:339–46.
19. Remy-Jardin M, Giraud F, Remy J, Copin MC, Gosselin B, Duhamel A. Importance of ground-glass attenuation in chronic diffuse infiltrative lung disease: pathologic–CT correlation. Radiology 1993;189:693–8.
20. Bouchardy LM, Kuhlman JE, Ball WC Jr, Hruban RH, Askin FB, Siegelman SS, et al. CT findings in bronchiolitis obliterans organizing pneumonia (BOOP) with radiographic, clinical and histologic correlation. J Comput Assist Tomogr 1993;17:352–7.
21. Müller NL, Guerry-Force ML, Staples CA, Wright JL, Wiggs B, Coppin C, et al. Differential diagnosis of bronchiolitis obliterans with organizing pneumonia and usual interstitial pneumonia: clinical, functional and radiologic findings. Radiology 1987;162:151–6.
22. Nicolaou S, Al-Nakshabandi NA, Müller NL. SARS: imaging of severe acute respiratory syndrome. AJR Am J Roentgenol 2003;180:1247–9.
23. McGuinness G, Scholes JV, Garay SM, Leitman BS, McCauley DI, Naidich DP. Cytomegalovirus pneumonitis: spectrum of parenchymal CT findings with pathologic correlation in 21 AIDS patients. Radiology 1994;192:451–9.
24. Müller NL, Ooi GC, Khong PL, Zhou LG, Tsang KW, Nicolaou S. High-resolution CT findings of severe acute respiratory syndrome at presentation and after admission. AJR Am J Roentgenol 2004;182:39–44.
25. Ketai LH. Conventional wisdom: unconventional virus. AJR 2009;193:1486–7.
26. Ketai L, Paul N, Wong K. Radiology of severe acute respiratory syndrome (SARS): the emerging pathologic–radiologic correlates of an emerging disease. J Thorac Imaging 2006;21:276–83.
27. Lee N, Hui D, Wu A, Chan P, Cameron P, Joynt GM, et al. A major outbreak of severe acute respiratory syndrome in Hong Kong. N Engl J Med 2003;348:1986–94.
28. Ujita M, Renzoni EA, Veeraraghavan S, Wells AU, Hansell DM. Organizing pneumonia: perilobular pattern at thin-section CT. Radiology 2004;232:757–61.
29. Gattinoni L, Bombino M, Pelosi P, Lissoni A, Pesenti A, Fumagalli R, et al. Lung structure and function in different stages of severe adult respiratory distress syndrome. JAMA 1994;271:1772–9.
30. Antonio GE, Wong KT, Hui DS, Wu A, Lee N, Yuen EH, et al. Thin-section CT in patients with severe acute respiratory syndrome following hospital discharge: preliminary experience. Radiology 2003;228:810–15.
31. Davies A, Jones D, Bailey M, Beca J, Bellomo R, Blackwell N, et al. Extracorporeal membrane oxygenation for 2009 influenza A(H1N1) acute respiratory distress syndrome. JAMA 2009;302:1888–95.
32. Goldstein I, Bughalo MT, Marquette CH, Lenaour G, Lu Q, Rouby JJ. Mechanical ventilation-induced air-space enlargement during experimental pneumonia in piglets. Am J Respir Crit Care Med 2001;163:958–64.
33. Xie L, Liu Y, Xiao Y, Tian Q, Fan B, Zhao H, et al. Follow-up study on pulmonary function and lung radiographic changes in rehabilitating severe acute respiratory syndrome patients after discharge. Chest 2005;127:2119–24.